APPLICATION OF NANOMATERIALS AND NANOTECHNOLOGIES IN CONSTRUCTION

Original article
https://doi.org/10.15828/2075-8545-2023-15-5-465-473

Peculiarities of the formation of silicon oxide films modified with metal nanoparticles

Vyacheslav I. Pavlenko, Andrey I. Gorodov*, Roman N. Yastrebinsky, Mikhail S. Lebedev, Vitaliy V. Kashibadze

Belgorod State Technological University Named after V.G. Shukhov, Belgorod, Russia

* Corresponding author: e-mail: gorodov-andreyy@mail.ru

ABSTRACT: Introduction. Silicon oxide film coatings have unique properties and are widely used in various industries, including construction. This paper presents the results on the preparation of polyalkylhydroxysiloxane liquid film in the presence of nanoscale particles of metallic bismuth. **Methods and materials.** Laser ablation method of metallic bismuth in aqueous medium was used to obtain bismuth nanoparticles. The surface of the target was treated with a laser beam at the workstation of an ytterbium pulsed fiber laser are discussed. The particle size and electrokinetic properties of colloidal bismuth sols were determined method by dynamic light scattering. After drying, Bi powder was added to polyalkylhydroxysiloxane liquid. Thin films cured under different heat treatment modes are applied to glass substrates by dipping. The resulting films were characterized by SEM, X-ray phase analysis, and FTIR spectroscopy. **Results.** In this work, the electrokinetic properties of colloidal bismuth sols are discussed. Laser ablation of a bismuth substrate leads to an increase in electrical conductivity and the appearance of a double electric layer in colloidal sols. The effect of the curing temperature on the properties of the coating is shown. It was found that the content of bismuth nanoparticles in the polyalkylhydroxysiloxane coating (3 wt.%) does not lead to the formation of crystalline phases. At the same time, the composition of the film and the mode of heat treatment affect the short-range order of molecular bonds. Increasing the content of bismuth nanoparticles in the coating of more than 10 wt.% leads to the appearance of microcrystalline phases of bismuth silicates in the system. **Conclusion.** The results obtained in the course of the study supplement the information about the production of bismuth nanoparticles by laser ablation and are of great importance in the practice of creating composite films.

KEYWORDS: polyorganohydrosiloxane, silicon dioxide, bismuth nanoparticles, laser ablation, electrokinetic potential, coatings, IR spectroscopy, bismuth silicates, silica-organic.

ACKNOWLEDGMENTS: This work was realized using the equipment of the High Technology Center at BSTU named after V.G. Shukhov, the framework of the State Assignment of the Ministry of Education and Science of the Russian Federation, project No. FZWN-2023-0004.

FOR CITATION: Pavlenko V.I., Gorodov A.I., Yastrebinsky R.N., Lebedev M.S., Kashibadze V.V. Peculiarities of the formation of silicon oxide films modified with metal nanoparticles. *Nanotechnologies in construction*. 2023; 15(5): 465–473. https://doi.org/10.15828/2075-8545-2023-15-5-465-473.– EDN: XUHDKC.

INTRODUCTION

Recently, scientists all over the world have paid much attention to the study of silica systems. This is due to the unique properties of silicon oxide-based materials and their wide application in various fields such as construction, optoelectronics, microelectronics, medicine, biology, energy, and the production of sensors [1].

One of the most common materials in modern industry is silicon oxide films. They offer high strength, corrosion and chemical resistance, as well as low production costs. In addition, silicon oxide films can be easily modified to achieve the desired properties, making them a versatile material for a variety of applications [2]. For example, to obtain promising materials for nonvolatile memory ReRAM (Resistive Random-Access Memory), thin films of amorphous SiO_x are implanted with nanoclusters of metallic zinc or its oxide [3–4]. In this case, crystalline phases of Zn content are formed in the amorphous silicon oxide film, which contributes to the manifestation of unique properties.

Among the methods for obtaining amorphous films of high purity silicon oxide, deposition from organic silicon compounds (silanes, silicon alkoxides, alkylhydroxysiloxanes) is widely used because of its simplicity and availability. The presence of Si-H reactive bonds in alkylhydroxysiloxanes makes them the most attractive for obtaining a wide range of coatings [5]. However, the composition and structure of films produced by high-temperature methods are highly dependent on the process temperature. Up to 700°C, the film is contaminated with organosilicon compounds due to incomplete decomposition. Above 750°C, the SiO_2 layer is contaminated with carbon, silicon carbide (SiC), and resinous pyrolysis products [6].

On the other hand, films of polycrystalline or monocrystalline silicon oxide [7] are of interest. It is known that the formation of crystalline silica from chemically pure amorphous SiO_2 occurs when heated to temperatures above 1200°C [8]. To obtain crystalline silicon oxide at lower temperatures, various methods are used: hydrothermal method [9], localized high-energy impact [10–11], polymer template creation [12] or inducing thin metal layer method [13–18], surface modification with nanoparticles [19–20], including core-shell structures [21]. At the same time, the crystallization processes of silicon oxide films are influenced by the substrate, for example, in epitaxy, the crystallographic orientation of the silicon substrate has a great influence, especially at relatively low temperatures [22–23]. The formation and growth of crystals on the plate with orientation (111) is better than with orientation (100). This dependence is explained by the fact that different crystallographic directions of the plate correspond to different number of Si–Si bonds.

There are some reports in the literature regarding a low temperature method of producing crystalline silica particles using metallic bismuth [18, 21]. The use of bismuth is justified by its low eutectic temperature, which reduces the thermal equilibrium of crystallization, as well as the high purity of the metal and the ease of its removal. There are also a large number of published works in which bismuth silicates are obtained in X-ray amorphous form [24–26].

This paper investigates the effect of the presence of different amounts of nanoscale bismuth particles obtained by laser ablation of metallic bismuth in aqueous medium on the formation and composition of a polyalkylhydroxysiloxane liquid film.

METHODS AND MATERIALS

The whole procedure for obtaining silicon oxide coatings modified with metallic nanoscale bismuth particles consists of several steps and is presented in Figure 1.

Nanoparticles (NPs) of metallic bismuth were prepared by ablation in aqueous medium [21]. The target in the form of Bi plates (frequency 99.999%), placed in a cuvette with distilled water at temperature T = 60°C, was subjected to high energy laser irradiation with constant stirring by a magnetic stirrer. The treatment of the target surface with the laser beam was carried out at the ytterbium pulsed fiber laser workstation (Minimarker 2-20 A4 PA, Russia) with the following parameters 1064 nm wavelength, frequency of 3 kHz, output power of 20 W. The pulse duration and laser exposure time were chosen to obtain the optimum particle size. The particle size was monitored using a device Zetatrac Microtrac Inc (USA), which works on the principle of dynamic light scattering. This instrument also provides information on the electrical conductivity and electrokinetic (ξ-) potential of the sols. In order to characterize freshly prepared Bi sols, the average value of 5 measurements was recorded, the discrepancy between the data for one object of study did not exceed 1%.

Then, the obtained sol was dried in air environment at 80°C, grayish white Bi powder was added to polyalkylhydroxysiloxane liquid (Point LLC, St. Petersburg, Russia) and thoroughly mixed. Glass plates were placed in the resulting suspension to form a film on them. The plates were then removed and heat-treated in a drying oven with continuous blowing of dilute argon to prevent spontaneous combustion. To study the influence of the curing conditions of the hydroxysiloxane polymer on the composition and microstructure of the coating, the samples

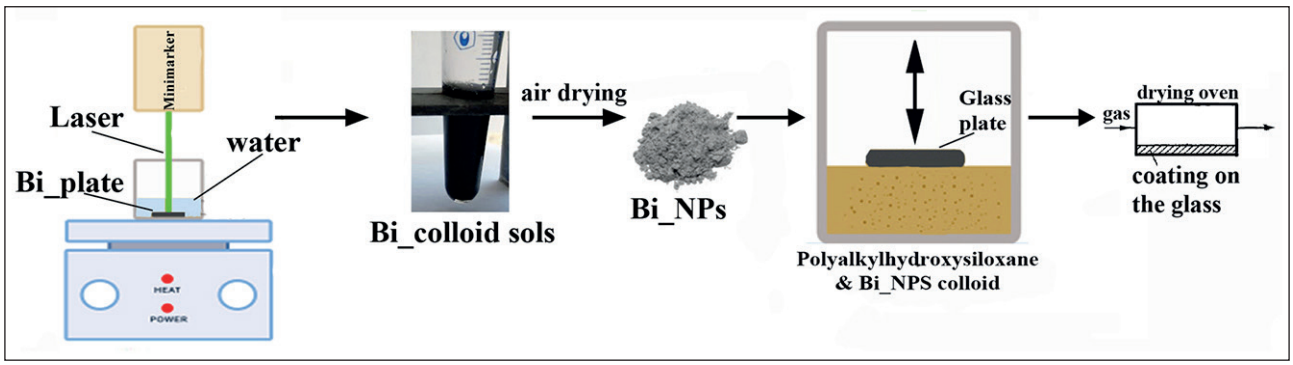

Fig. 1. **Scheme for obtaining silicon oxide films modified with bismuth nanoparticles**

Table 1
Electrical conductivity and ζ-Potential of Bi sols obtained under different laser ablation modes.

	Value		
Laser exposure mode	P = 4 ns, t = 7 min	P = 8 ns, t = 7 min	P = 8 ns, t = 15 min
Conductivity, μS/cm	225	297	293
ζ-Potential, mV	+11.2	+14.5	+14.8

were subjected to heat treatment with a smooth mode of temperature rise to 300–500°C and holding at a given temperature for 1.5 hours.

Glass substrates with the obtained coating were examined by scanning electron microscopy (SEM) on a TESCAN MIRA 3LMU instrument with energy dispersive X-ray spectra (EDS) at different points (microareas) using an integrated X-MAX 50 Oxford Instruments spectrometer (TESCAN ORSAY HOLDING, Czech Republic).

X-ray diffraction (XRD) patterns of the coatings were recorded using a diffractometer ARL X'TRA (Thermo Fisher Scientific, USA) with a CuKα source in the range of 2θ angles from 4° to 64° in the asymmetric coplanar imaging mode with a sliding angle of incidence α = 3° (θ-scan) [7]. Phase analysis was performed with Crystallographica Search-Match version 2.0.3.1 software using data (PDF-4) from the JCPDS International Centre for Diffraction Data.

IR spectra of light absorption were recorded on a VERTEX 70 (Bruker Optics GmbH) Fourier transform spectrometer in the 4000–400 cm^{-1} wave number range. For this purpose, the coating sample was ground with potassium bromide (1:100) in an agate mortar and translucent tablets were obtained using a hydraulic press.

RESULTS AND DISCUSSION

As a result of laser ablation of bismuth plate in aqueous medium at varying pulse duration (P) and exposure time (t), colloidal sols of light gray to dark brown color were obtained. The data of differential particle size distribution of the obtained sols are shown in Figure 2. The obtained bismuth particles have nanometer size in all investigated modes of laser exposure. However, the Bi NPs obtained by ablation at pulse duration P = 4 ns are characterized by a broader particle size distribution compared to the mode P = 8 ns, in which more homogeneous particles with an average diameter of 13...14 nm were obtained. In general, the sols obtained have a relatively low stability and the particles sediment in aqueous medium after several hours.

The conductivity and ζ-potential data of freshly prepared Bi sols (Table 1) may indicate the formation of carbonate phases from aqueous air microbubbles during target ablation, since bismuth has a high affinity for carbon [24, 27]. The electrical conductivity of distilled water in the presence of bismuth plate before laser treatment

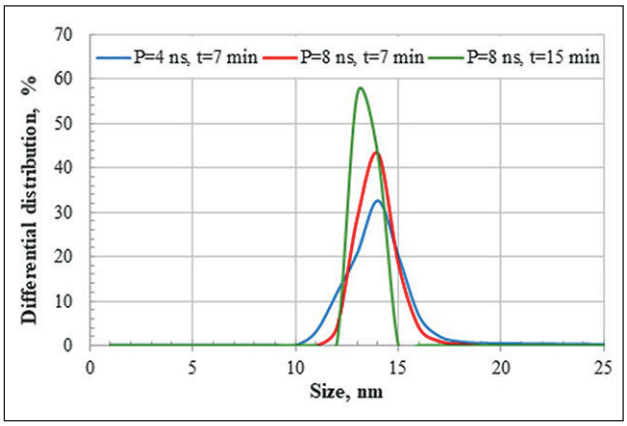

Fig. 2. **Differential distribution of Bi particles by size obtained under different modes of laser exposure**

was also determined, which was 5 μS/cm. The increase in electrical conductivity after laser ablation proves the presence of ions in the colloidal sols, which provides the appearance of the electric double layer (EDL) and the slip boundary potential. Based on the obtained data and the information available in the literature about the formation of bismuth subcarbonate during laser ablation in aqueous medium [24], an assumption was made about the structure of the micelles, which can be described by the formula:

$$\left\{m\,[Bi]\cdot n\ BiO^{+}\cdot(n-x)\ HCO_3^{-}\right\}^{x-}\cdot x\ HCO_3^{-}.$$

Relatively low absolute values of ζ-Potential (less than 25 mV) do not provide high stability of the studied disperse systems by electrokinetic factor.

Figure 3 (a) shows the structure of SiO_2 film with embedded Bi NPs cured at 400°C on the glass surface. The formed coating consists of a continuous film firmly adhered to the surface of the glass substrate. The thickness of the film is ~1 μm. The surface of the coating contains localized small particles of Bi/SiO_2. The elemental chemical composition of the coating has been verified by EDS measurements in the cross section Figure 3 (b, c). A continuous silica-containing layer and embedded small Bi particles (bright areas) can be seen. The size of the bismuth particles in the layer is larger than the average size of the NPs obtained by laser ablation, which is due to their agglomeration.

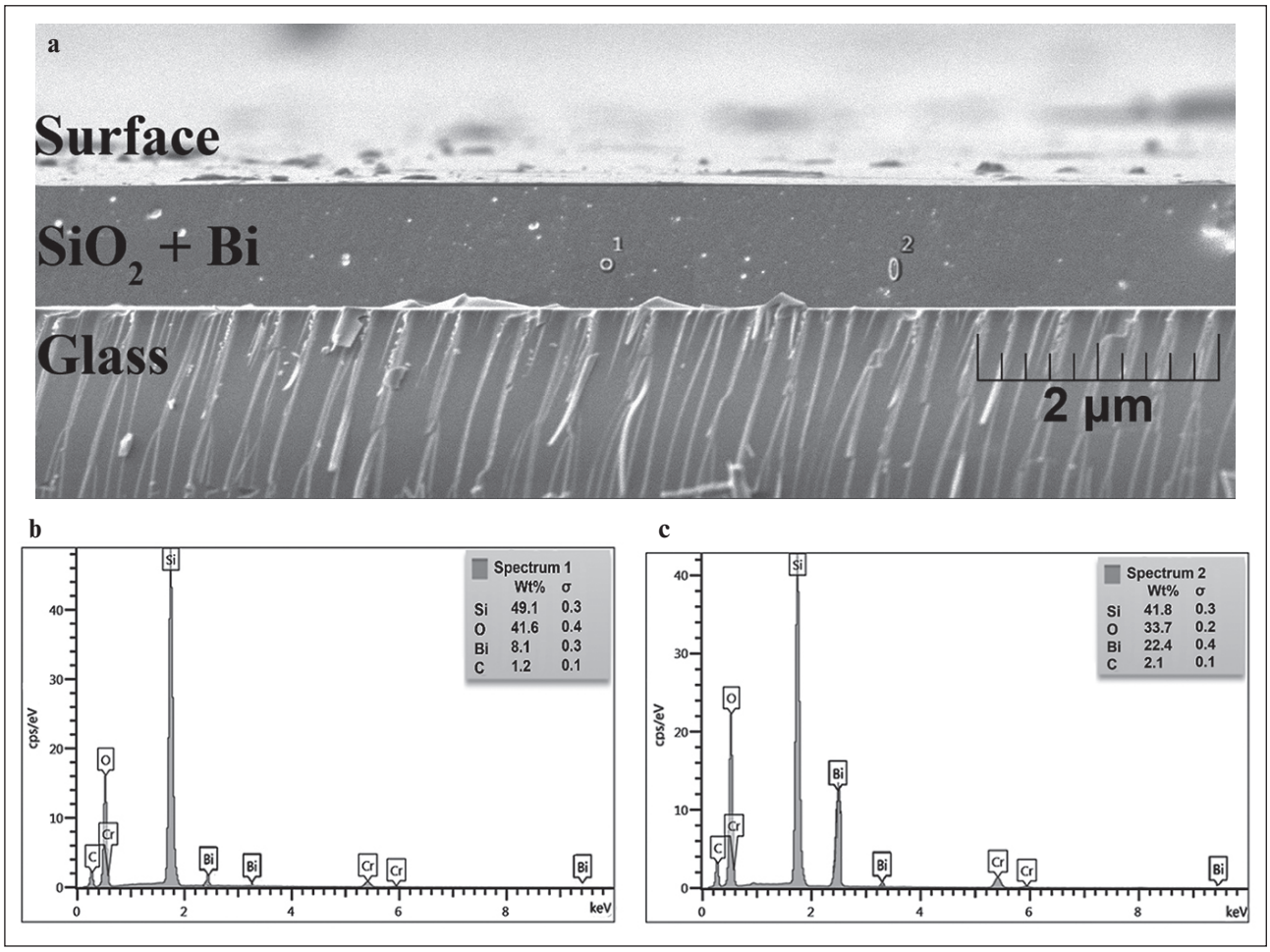

Fig. 3. **SEM images of (side view) SiO_2 films with embedded Bi NPs, harden at 400°C (a), EDS spectrum in Point 1 (b) and Point 2 (c)**

Increasing the curing temperature up to 500°C leads to film fracture and appearance of a large number of microcracks. However, despite cracking, the coating has a tight contact with the substrate Figure 4. The appearance of microcracks in the coating is due to the redistribution of molecules and changes in the film density.

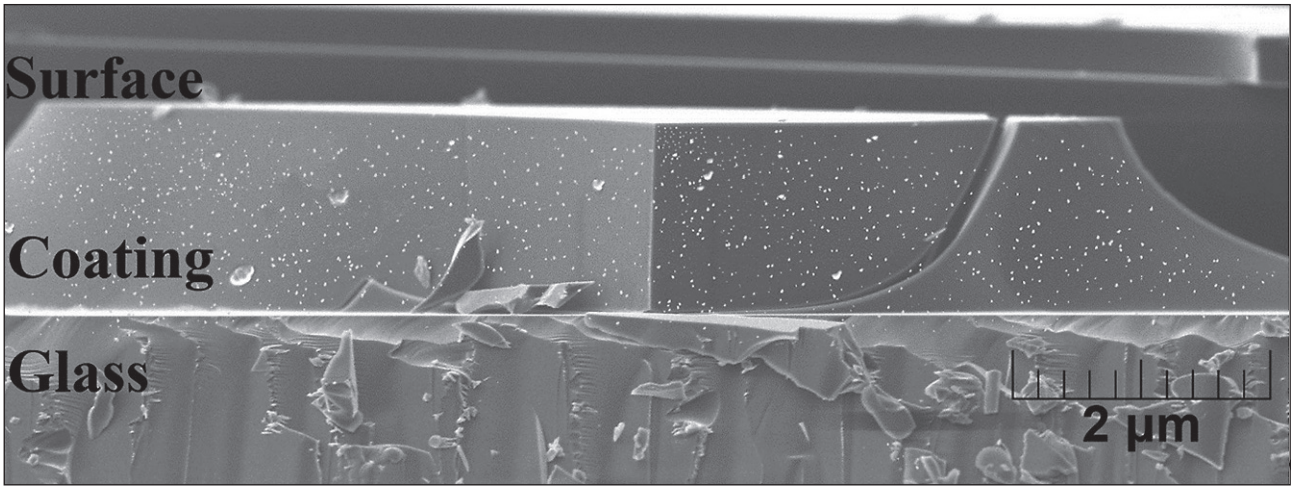

Fig. 4. **SEM images of (side view) SiO_2 films with embedded Bi NPs, cured at 500°C**

FT-IR spectra of samples with different compositions cured at different temperatures were taken to study the details of the interaction of the components during coating formation (Figures 5–6).

The spectrum of the coating obtained from pure polyalkylhydroxysiloxane at 400°C (Figure 5a) contains bands characteristic of amorphous silica [6].

The absorption bands with a peak at 460 cm^{-1} corresponds to the stretching δ- vibrations of the Si–O bonds of the SiO_4 tetrahedron. This band is characteristic of all samples and all modifications of SiO_2, so it is used as an average standard.

Broad bands at 660–890 and 890–1200 cm^{-1} are associated with symmetric ϑ_s and asymmetric ϑ_{as} vibrations of Si–O bonds.

It can be seen that the bands are very close to each other and overlap. A change in the shape of the broad spectra is observed when the composition and temperature treatment mode of the samples are changed. Therefore, the spectra were decomposed into Gaussian curves for a more detailed evaluation of the redistribution of band intensities and molecular rearrangement. The sum line (Fit Sum) of all Gaussians almost repeats the line of the original IR spectrum. The legend of each Gaussian curve gives the coordinates of the peak apex: wavenumber (cm^{-1}) and absorption intensity. Splitting the absorption bands into Gaussians allows us to see the presence of several structural types of molecular phases.

Thus, the broad band in the 660–890 cm^{-1} region can be decomposed into three Gaussian curves. For example,

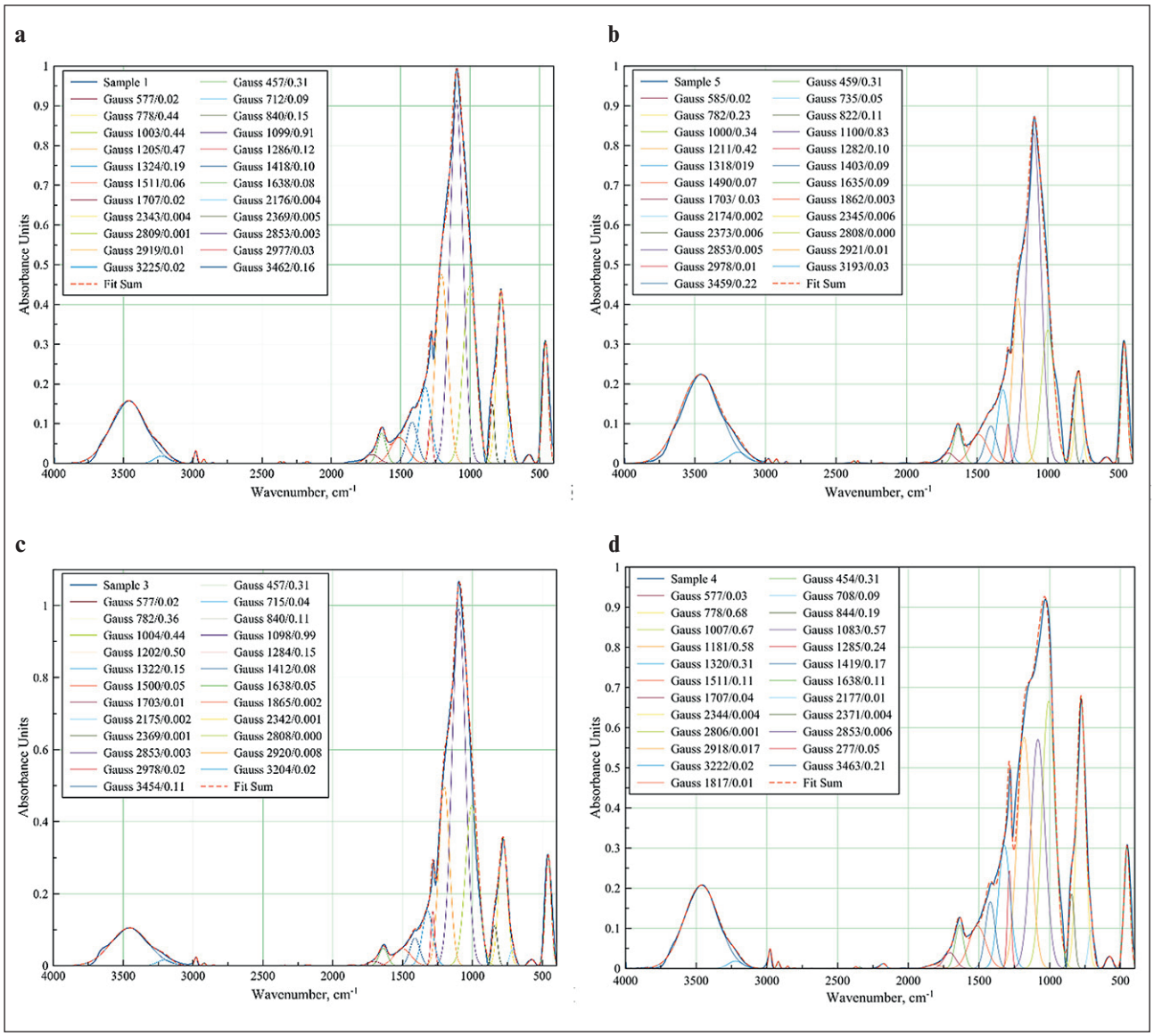

Fig. 5. **FT-IR spectra of films of different compositions cured at 400°C:** 100% polyalkylhydroxysiloxane (a); 0.5 wt.% Bi NPs (b); 1 wt.% Bi NPs (c); 3 wt.% Bi NPs (d)

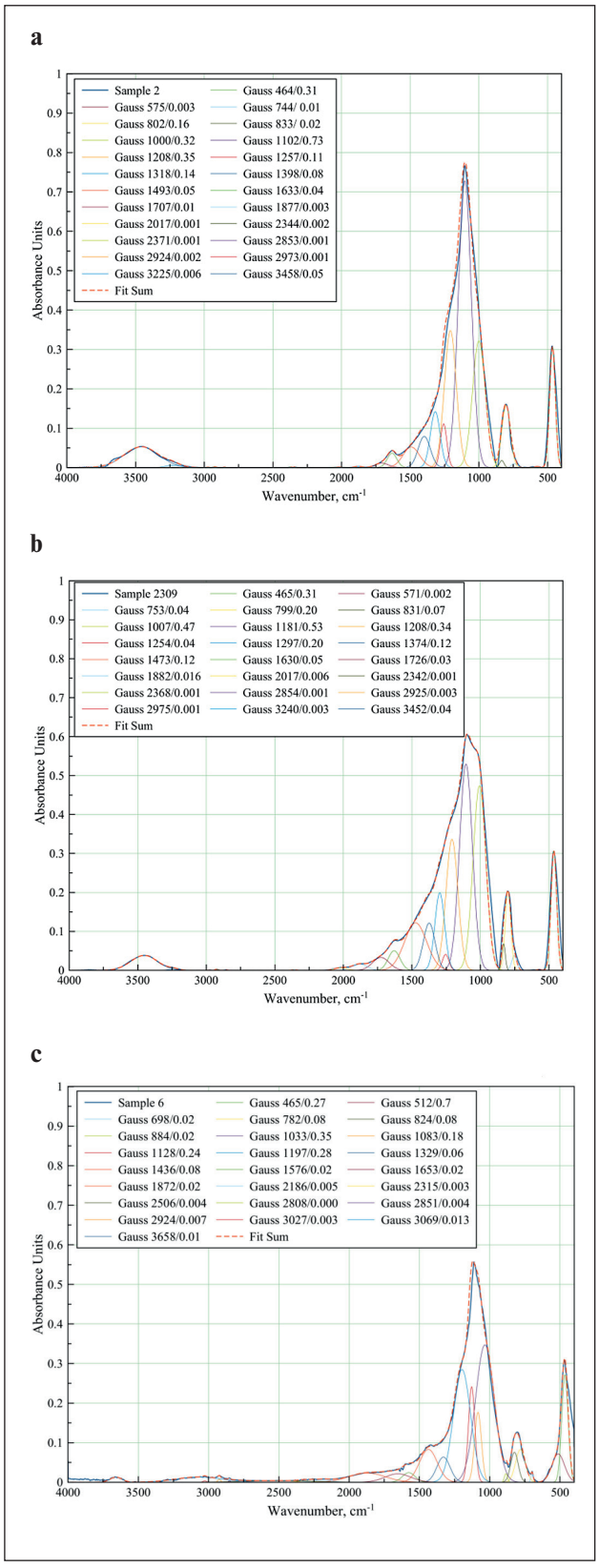

Fig. 6. **FT-IR spectra of films of different compositions cured at 500°C:** 100% polyalkylhydroxysiloxane (a); 3 wt.% Bi NPs (b); 10 wt.% Bi NPs (c)

in a sample of pure polyalkylhydroxysiloxane heat-treated at 400°C (Figure 5a), these curves are characterized by peaks at 712, 778, and 840 cm^{-1}. The Gaussian peak at 712 cm^{-1} seems to be related to the incomplete decomposition of organic compounds, since it shifts to the high frequency region up to 744 cm^{-1} after heat treatment (Figure 6a). The introduction of bismuth particles into the sample also shifts this Gaussian (Figure 5b-d), which is associated with the superposition of strain vibration bands for the Si–O–Bi bond. The Gaussians at 778 and 840 cm^{-1} are more stable with the introduction of NPs Bi, the peak is practically not shifted, only the intensity changes: the intensity increases with increasing Bi content (Figure 5b–d). However, heat treatment at 500°C slightly shifts these peaks to 800 and 830 cm^{-1}, respectively (Figure 6b). In the literature, these wavenumbers characterize the symmetric valence vibrations of Si–O and Si–OH bonds [6].

Gaussians at 1000, 1100 and 1200 cm^{-1} belong to the band of asymmetric valence vibrations of the Si–O–Si bond of SiO_4 tetrahedrons. With increasing Bi content in the samples, the intensity of these Gaussians increases (Figure 5), but unevenly: the Gaussian with the peak at 1000 cm^{-1} increases more. This affects the change in shape of the overall peak. Obviously, the data obtained indicate certain changes in the structure of the arrangement of molecules in the short-range order.

The band in the range of 540–620 cm^{-1} is observed in all samples heat-treated at 400°C (Figure 5) and can be attributed to the C–H bond. This indicates incomplete decomposition of polyalkylhydroxysiloxane under these heat treatment conditions. Those heat-treated at 500°C showed no peak in the 540–620 cm^{-1} region (Figure 6a–b). The same is true for the 1286 cm^{-1} band corresponding to the Si–CH_3 bond. However, it can be observed that as the content of Bi NPs increases in the samples heat-treated at 400°C, the intensity of the ~1283 cm^{-1} band also increases, indicating an increase in the proportion of hydrocarbon residue in the product.

A weak band at 1832–1872 cm^{-1}, caused by symmetric distortion and stretching of Si–O bonds, was observed in the samples with the addition of Bi NPs. This band was not detected in the polyalkylhydroxysiloxane samples.

Despite the relatively high treatment temperature (400°C), water is present in all samples (Figure 5), which is confirmed by the presence of absorption bands in the region of 1630 cm^{-1} (deformation vibrations of water molecules), 2808–2850 cm^{-1} (associated with hydrogen bonds), 3100–3600 cm^{-1} (O–H vibrations in the water molecule). Treatment at 500°C (Figure 6a–b) reduces the intensity of the bands characteristic of water molecule vibrations but does not eliminate them completely.

Since the small number of Bi nanoparticles (up to 3 wt.%) in the sample does not allow the identification of separate bands characteristic of bismuth bond vibrations,

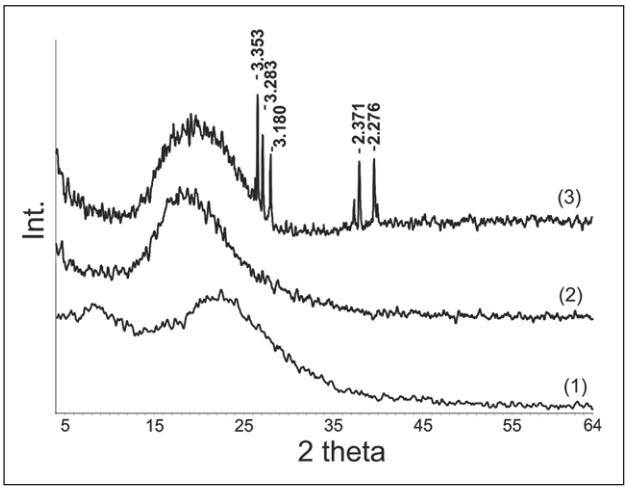

Fig. 7. **XRD pattern of coating:** 1 – polyalkylhydroxysiloxane; 2 – 3 wt.% Bi NPs; 3 – 10 wt.% Bi NPs

IR spectra of the sample containing 10 wt.% Bi NPs were recorded (Figure 6c). It can be seen that the band with the peak at 466 cm^{-1}, corresponding to δ-vibrations of Si–O bonds, is broadened and overlaps with the band in the region of 510–540 cm^{-1}, characterizing the deformation vibrations of Si–O–Bi. Weak bands at 698 cm^{-1} (caused by Bi–O bond vibrations in BiO_3 and BiO_6 structural units) and 884 cm^{-1} (Si–O–Bi vibrations) are also observed [28].

X-ray diffraction (XRD) was used to investigate the presence of crystalline phases (Figure 7).

The X-ray diffraction results indicate that the coating obtained from pure polyalkylhydroxysiloxane, regardless of the temperature regime of processing, is characterized by a completely amorphous structure. This is confirmed by the presence of an amorphous halo in the range of angles 2θ 10–20° on the XRD. When obtaining a polyalkylhydroxysiloxane coating with the addition of Bi NPs (up to 3 wt.%), a broadening of the amorphous halo is observed, which may be due to the presence of traces of the fine crystalline phase. The higher content (10 wt.%) of bismuth nanoparticles in the coating leads to the appearance of peaks in the XRD, which proves the presence of microcrystalline phases of bismuth silicates in the system.

CONCLUSION

Nanometer-sized particles have been obtained by laser ablation of metallic bismuth in aqueous medium. It is shown that laser ablation of bismuth contributes to obtaining a sol in which an electric double layer (EDL) and a slip boundary potential appear. However, the bismuth sols obtained are not characterized by stability on the electrokinetic factor.

The possibility of obtaining a film from polyalkylhydroxysiloxane liquid in the presence of nano-sized bismuth particles has been established. At optimum temperature mode of drying (up to 400°C), despite the aggregation of bismuth particles, it is possible to obtain a film that is continuous, uniform, and tightly adhering to the surface of the glass substrate.

The detailed analysis of IR spectra of coatings with different contents of bismuth nanoparticles showed that the small number of NPs Bi added (up to 3 wt.%) and the heat treatment mode affect the short-range order of molecular bonds. However, absorption bands characteristic of crystalline silicate phases do not appear. Increasing the content of bismuth nanoparticles in the coating up to 10 wt.% contributes to the appearance of bands characterizing the deformation vibrations of Si–O–Bi and vibrations of Bi–O bonds in BiO_3 and BiO_6 structural units.

The X-ray phase analysis confirmed the IR spectroscopy data that the content of bismuth nanoparticles in the polyalkylhydroxysiloxane coating of more than 10 wt.% leads to the appearance of microcrystalline phases of bismuth silicates in the system. When introducing a small amount of bismuth (3 wt.%) the formation of crystalline phases does not occur.

REFERENCES

1. Valtchev V.P., Faust A.C., Lézervant J. Rapid synthesis of silicalite-1 nanocrystals by conventional heating. *Microporous and Mesoporous Materials*. 2004; 68: 91-95. https://doi.org/10.1016/j.micromeso.2003.11.018

2. Post P., Wurlitzer L., Maus-Friedrichs W., Weber A.P. Characterization and applications of nanoparticles modified in-flight with silica or silica-organic coatings. *Nanomaterials*. 2018; *8*(7): 530. https://doi.org/10.3390/nano8070530

3. Privezentsev V.V., Kulikauskas V.S., Zatekin V.V., Kiselev D.A., Voronova M.I. Study of Memristors Based on Silicon Oxide Films Implanted with Zn. *Poverkhnost. Rentgenovskie, Sinkhrotronnye i Neitronnye Issledovaniya*. 2022; 6: 96-102. https://doi.org/10.31857/S1028096022060140

4. Privezentsev V.V., Sergeev A.P., Firsov A.A., Kulikauskas V.S., Yakimov E.E., Kirilenko E.P., Goryachev A.V. Study of Zn implanted silicon oxide films. *Physics of the Solid State*. 2023; 4: 679-684. https://doi.org/10.21883/PSS.2023.04.56013.17

5. Pakuła D., Marciniec B., Przekop R.E. Direct Synthesis of Silicon Compounds—From the Beginning to Green Chemistry Revolution. *AppliedChem* 2023; 3: 89-109. https://doi.org/10.3390/appliedchem3010007

6. Pavlenko V.I., Cherkashina N.I., Edamenko O.D., Yastrebinsky R.N., Noskov A.V., Prokhorenkov D.S., Gorodov A.I., Piskareva A.O. Synthesis and Characterization of Silicon–Carbon Powder and Its Resistance to Electron Irradiation. *Journal of Composites Science*. 2023; 7: 340. https://doi.org/10.3390/jcs7080340

7. Cherkashina, N.I.; Pavlenko, V.I.; Zaitsev, S.V.; Gorodov, A.I.; Domarev, S.N.; Sidelnikov, R.V.; Romanyuk, D.S. Adhesion Strength of Al, Cr, In, Mo, and W Metal Coatings Deposited on a Silicon–Carbon Film. *Coatings* 2023; 13: 1353. https://doi.org/10.3390/coatings13081353

8. Skorodumova O.B., Semchenko G.D., Goncharenko Y.N., Tolstoj V.S. Crystallization of SiO_2 from ethylsilicate-based gels. *Steklo i Keramika*. 2001; 74(1): 31-33. https://doi.org/10.1023/a:1010933028152

9. Oehler J.H. Hydrothermal crystallization of silica gel. *Geological Society of America Bulletin*. 1976; 87: 1143-1152. https://doi.org/10.1130/0016-7606(1976)87%3C1143:HCOSG%3E2.0.CO;2

10. Kishore R., Sood K., Naseem H. Microstructural and analytical investigation of low temperature crystallized amorphous silicon/crystallized silicon interface using SEM and EDS. *Journal of Materials Science Letters*. 2002; 21: 647-648. https://doi.org/10.1023/A:1015600423981

11. Kioseoglou J., Komninou P., Dimitrakopulos G.P., Antoniades I. P., Hatalis M. K., Karakostas Th. Crystallization of amorphous silicon thin films: comparison between experimental and computer simulation results. *Journal of Materials Science*. 2008; 43: 3976–3981. https://doi.org/10.1007/s10853-007-2226-1

12. Huang J., Zhang P., Wang X., Luo L., Gao J., Peng C., Liu X. Crystallization of inorganic silica based on interaction between polyimide and silica by sol–gel method. *Journal of Sol-Gel Science and Technology*. 2013; 66: 193–198. https://doi.org/10.1007/s10971-013-2989-6

13. Nast O., Brehme S., Neuhaus D.H., Wenham S. R. Polycrystalline silicon thin films on glass by aluminum-induced crystallization. *IEEE Transactions on Electron Devices*. 1999; 10: 2062-2068. https://doi.org/10.1109/16.791997

14. Hossain M., Meyer H.M., Abu-Safe H.H., Naseem H., Brown W.D. Large-grain poly-crystalline silicon thin films prepared by aluminum-induced crystallization of sputter-deposited hydrogenated amorphous silicon. *Journal of Materials Research*. 2006; 21: 761–766. https://doi.org/10.1557/jmr.2006.0091

15. Schneider J., Schneider A., Sarikov A., Klein J., Muske M., Gall S., Fuhs W. Aluminum-induced crystallization: Nucleation and growth process. *Journal of Non-Crystalline Solids*. 2006; 352(9-20): 972-975. https://doi.org/10.1016/j.jnoncrysol.2005.09.036

16. Knaepen W., Detavernier C., Van Meirhaeghe R.L., Jordan Sweet J., Lavoie C. In-situ X-ray Diffraction study of Metal Induced Crystallization of amorphous silicon. *Thin Solid Films*. 2008; 516(15): 4946-4952. https://doi.org/10.1016/j.tsf.2007.09.037

17. Wang T., Yan H., Zhang M., Song X., Pan Q., He T., Hu Z., Jia H., Mai Y. Polycrystalline silicon thin films by aluminum induced crystallization of amorphous silicon. *Applied Surface Science*. 2013; 264: 11-16. https://doi.org/10.1016/j.apsusc.2012.09.019

18. Zouini M., Ouertani R., Amlouk M., Dimassi W. Annealing Temperature Effect on Bismuth Induced Crystallization of Hydrogenated Amorphous Silicon Thin Films. *Silicon*. 2022; 14: 2115–2125. https://doi.org/10.1007/s12633-021-01005-7

19. Kaito C., Kumamoto A., Saito Y., Ono R. Low-temperature crystallization of thin silicate layer on crystalline Fe dust. *Earth, planets and space*. 2010; 62: 29–31. https://doi.org/10.5047/eps.2008.10.002

20. Wang W., Huang J., Lu Y., Yang Y., Song W., Tan R., Dai S., Zhou J. In situ micro-Raman spectroscopic study of laser-induced crystallization of amorphous silicon thin films on aluminum-doped zinc oxide substrate. *J Mater Sci: Mater Electron*. 2012; 23: 1300–1305. https://doi.org/10.1007/s10854-011-0588-2

21. Hassan S.S., Hubeatir K.A., Al-haddad R.M.S. Characterization and antibacterial activity of silica-coated bismuth ($Bi@SiO_2$) nanoparticles synthesized by pulsed laser ablation in liquid. *Optik (Stuttg)*. 2023; 273: 170453. https://doi.org/10.1016/j.ijleo.2022.170453

22. Song Y.H., Kang S.Y., Cho K.I., Yoo H.J., Kim J.H., Lee J.Y. Polycrystalline Silicon Films Formed by Solid-Phase Crystallization of Amorphous Silicon: The Substrate Effects on Crystallization Kinetics and Mechanism. *MRS Online Proceedings Library*. 1996; 424: 243–248. https://doi.org/10.1557/PROC-424-243

23. Kioseoglou J., Komninou P., Dimitrakopulos G.P., Antoniades I.P., Hatalis M.K., Karakostas T. Crystallization of amorphous silicon thin films: comparison between experimental and computer simulation results. *J Mater Sci*. 2008; 43: 3976–3981. https://doi.org/10.1007/s10853-007-2226-1

24. Golubovskaya A.G., Fakhrutdinova E.D., Svetlichnyi V.A. Bismuth silicates: preparation by pulsed laser ablation and photocatalytic activity. *Proc. SPIE 12086, XV International Conference on Pulsed Lasers and Laser Applications*. 2021: 120861Y. https://doi.org/10.1117/12.2612743

25. Belik Y.A., Vodyankin A.A., Fakhrutdinova E.D., Svetlichnyi V.A., Vodyankina O.V. Photoactive bismuth silicate catalysts: Role of preparation method. *Journal of Photochemistry and Photobiology A: Chemistry*. 2022; 425: 113670. https://doi.org/10.1016/j.jphotochem.2021.113670

26. Shabalina A.V., Fakhrutdinova E.D., Golubovskaya A.G., Kuzmin S.M., Koscheev S.V., Kulinich S.A., Svetlichnyi V.A., Vodyankina O.V. Laser-assisted preparation of highly-efficient photocatalytic nanomaterial based on bismuth silicate. *Applied Surface Science*. 2022; 575: 151732. https://doi.org/10.1016/j.apsusc.2021.151732

27. Ortiz-Quiñonez J.L., Vega-Verduga C., Díaz D., Zumeta-Dubé I. Transformation of Bismuth and β-Bi_2O_3 Nanoparticles into $(BiO)_2CO_3$ and $(BiO)_4(OH)_2CO_3$ by Capturing CO_2: The Role of Halloysite Nanotubes and "Sunlight" on the Crystal Shape and Size. *Crystal Growth & Design*. 2018; *18*(8): 4334-4346. https://doi.org/10.1021/acs.cgd.8b00177

28. Yastrebinskii R.N., Pavlenko A.V., Bondarenko G.G. Structural Features of Mineral Crystalline Phases and Defectiveness of Bismuth Organosiliconate Crystals at High Temperatures. *Inorganic Materials: Applied Research*. 2018; 9(5): 825-831. https://doi.org/10.1134/S2075113318050313

INFORMATION ABOUT THE AUTHORS

Vyacheslav I. Pavlenko – Dr. Sci. (Eng.), Professor, Head of the Department of "Theoretical and Applied Chemistry", Belgorod State Technological University named after V.G. Shukhov, Belgorod, Russia, belpavlenko@mail.ru, https://orcid.org/0000-0002-3464-1880

Andrey I. Gorodov – Cand. Sci. (Eng.), Associate Professor, Department of "Theoretical and Applied Chemistry", Belgorod State Technological University named after V.G. Shukhov, Belgorod, Russia, gorodov-andreyy@mail.ru, https://orcid.org/0000-0002-5530-3282

Roman N. Yastrebinsky – Dr. Sci. (Eng.), Director of the Institute of Chemical Technology, Belgorod State Technological University named after V.G. Shukhov, Belgorod, Russia, yrndo@mail.ru, https://orcid.org/0000-0002-6413-0002

Mikhail S. Lebedev – Senior Researcher, Department of "Theoretical and Applied Chemistry", Belgorod State Technological University named after V.G. Shukhov, Belgorod, Russia; Scientific and Educational Center "Additive technologies", National Research Tomsk State University, Tomsk, Russia, michaell1987@yandex.ru, https://orcid.org/0000-0003-3194-9238

Vitaliy V. Kashibadze – Postgraduate student, Department of "Theoretical and Applied Chemistry", Belgorod State Technological University named after V.G. Shukhov, Belgorod, Russia, vitaliy.kashibadze@mail.ru, https://orcid.org/0000-0003-2246-6605

CONTRIBUTION OF THE AUTHORS

Vyacheslav I. Pavlenko – scientific guidance, setting research goals and objectives, formal analysis of research results.

Andrey I. Gorodov – conducting the experimental part of the study, analyzing the results of the study, writing the original text of the article.

Roman N. Yastrebinsky – development of research methodology, research concept, revision of the text of the article.

Mikhail S. Lebedev – conducting the experimental part of the study, processing the results of the study.

Vitaliy V. Kashibadze – conducting the experimental part of the study, data processing, editing.

The authors declare no conflicts of interests.

The article was received by the editors 01.09.2023; approved after peer review 05.10.2023; accepted for publication 10.10.2023.